

Design and Control of Vehicle Boom Barrier Gate system using Augmented H_2 Optimal and H_∞ Synthesis Controllers

¹Mustefa Jibril, ¹Messay Tadesse and ²Tesfabirhan Shoga

¹*School of Electrical and Computer Engineering, Dire Dawa Institute of Technology, Dire Dawa, Ethiopia*

²*Faculty of Electrical and Computer Engineering, Jimma Institute of Technology, Jimma, Ethiopia*

Key words: Boom barrier gate, H_2 optimal, H_∞ synthesis

Corresponding Author:

Mustefa Jibril

School of Electrical and Computer Engineering, Dire Dawa Institute of Technology, Dire Dawa, Ethiopia

Page No.: 172-177

Volume: 16, Issue 5, 2021

ISSN: 1816-949x

Journal of Engineering and Applied Sciences

Copy Right: Medwell Publications

Abstract: A vehicle boom barrier gate system is one of the recently developed technologies operating at the entrances to the restricted areas. This study aims to design and control of vehicle's boom barrier gate system using robust augmentation technique. H_2 optimal and H_∞ synthesis controllers are used to improve the performance of the system. The open loop response analysis of the vehicle boom barrier gate system shows that the input of the system need to be improved. Comparison of the vehicle boom barrier gate system with H_2 optimal and H_∞ synthesis controllers have been done to track a set point desired angular position using a step and operational open and close input signals and a promising results have been observed.

INTRODUCTION

A vehicle boom barrier gate system, is a bar, or beam pivoted to allow the boom to block vehicular or passer-by entrees through a controlled point. Typically, the tip of a boom entrance rises in a normal arc to a near regular position. Boom barrier gates are often counter weighted, so the pole is easily tipped. Boom barrier gates are often paired either conclusion to end, or offset appropriately to block entrance in both directions. Some boom gates also have a helper arm which hangs 300-400 mm below the upper tongs when lowered, to supplement approach visibility and which hangs on links so it lies flat with the main boom as the limit is raised. Some limit also features a pivot roughly half way, whereas the limit is raised, the outermost half remains horizontal, with the limit resembling an upside-down L when raised. Boom barrier gates are typically found at tier crossings, drawbridges, parking facilities, checkpoints and doorway to restricted areas. They are also the usual bureau for

controlling ducts through toll booths and tins also be found on some freeway entryways levee which are automatically controlled to drop to restrict traffic in the demand of incident washing or progress closures without the poverty to dispatch lane laborer or direction enforcement to use a means to block the way. Some boom barrier gates are automatic and powered, others are manually operated. Manual gates are sometimes hung in the manner of a usual gate (i.e., hinged horizontally). In some places, boom barrier gates are installed across suburban streets as a traffic calming measure, obstacle through traffic while allowing authorized vehicles such as emergency services and buses to take advantage of the shorter and more direct route^[1].

MATERIALS AND METHODS

Mathematical modeling of vehicle boom barrier gate system: The vehicle boom barrier gate system design is shown in Fig. 1.

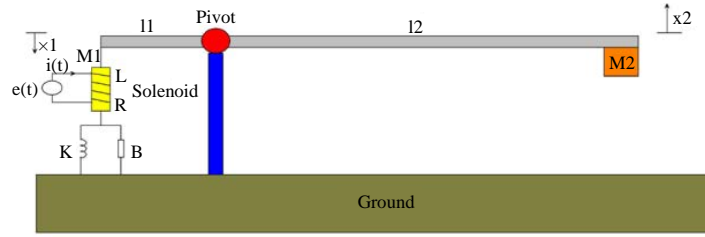


Fig. 1: Vehicle boom barrier gate system design

For the solenoid system we have:

$$Ri(t) + L \frac{di(t)}{dt} = e(t) \quad (1)$$

We assume that the solenoid produces a magnetic force proportional to the current in the coil^[2]:

$$f = K_i i(t) \quad (2)$$

The equilibrium equation of the arm is given as:

$$\frac{x_1}{x_2} = \frac{f_1}{f_2} = \frac{l_1}{l_2} \quad (3)$$

The force equation at point 2 is:

$$f_2 = M_2 \frac{d^2 x_2}{dt^2} \quad (4)$$

The force equation at point 1 is:

$$M_1 \frac{d^2 x_1}{dt^2} + B \frac{dx_1}{dt} + Kx_1 + f_1 = f \quad (5)$$

Substituting Eq. 2 for f and Eq. 3 for f_1 to Eq. 5 yields:

$$M_1 \frac{d^2 x_1}{dt^2} + B \frac{dx_1}{dt} + Kx_1 + f_2 \frac{l_1}{l_2} = K_i i(t) \quad (6)$$

Again substituting Eq. 3 for x_1 and Eq. 4 for f_2 to Eq. 6 yields:

$$\left(M_1 \frac{l_1}{l_2} + M_2 \frac{l_1}{l_2} \right) \frac{d^2 x_2}{dt^2} + B \frac{l_1}{l_2} \frac{dx_2}{dt} + K \frac{l_1}{l_2} x_2 = K_i i(t) \quad (7)$$

Taking the Laplace transform of Eq. 7 yields:

$$\left(\left(M_1 \frac{l_1}{l_2} + M_2 \frac{l_1}{l_2} \right) s^2 + B \frac{l_1}{l_2} s + K \frac{l_1}{l_2} \right) X_2(s) = K_i I(s) \quad (8)$$

Table 1: System parameters

Parameters	Symbols	Values
Side 1 rod length	l_1	1 (m)
Side 2 rod length	l_2	3.75 (m)
Mass of solenoid	M_1	2 (kg)
Mass at the rod side 2	M_2	3.5 (kg)
Spring stiffness	K	38 (N/m)
Damping coefficient	B	18 (N-s/m)
Resistance	R	75 (Ω)
Inductance	L	15 (h)
Magnetic force constant	K_i	0.014

Taking the Laplace transform of Eq. 1 and substituting it into Eq. 8 for $i(t)$ yields:

$$\left(\left(M_1 \frac{l_1}{l_2} + M_2 \frac{l_1}{l_2} \right) s^2 + B \frac{l_1}{l_2} s + K \frac{l_1}{l_2} \right) X_2(s) = K_i \frac{E(s)}{(R + Ls)} \quad (9)$$

The transfer function between the input voltage and the output displacement becomes:

$$\frac{X_2(s)}{E(s)} = \frac{\left(\frac{l_2}{l_1} \right) K_i}{(M_1 + M_2)Ls^3 + ((M_1 + M_2)R + BL)s^2 + (BR + KL)s + KR} \quad (10)$$

The angular position at point 2 is simply:

$$X_2(s) = \frac{2\pi l_2}{360} \theta_2(s) \quad (11)$$

Substituting Eq. 11 in to Eq. 10 yields to the transfer function between the input voltage and the output angular displacement as^[3]:

$$\frac{\theta_2(s)}{E(s)} = \frac{\frac{180}{\pi l_1} K_i}{(M_1 + M_2)Ls^3 + ((M_1 + M_2)R + BL)s^2 + (BR + KL)s + KR}$$

The system parameters are given in Table 1. Numerically the transfer function becomes^[4]:

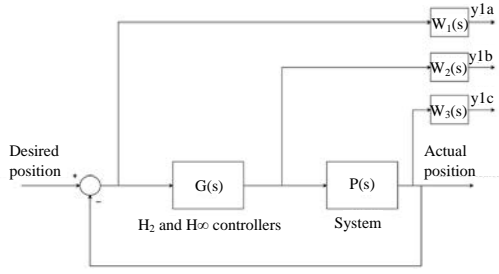


Fig. 2: Weighted control structure with the proposed controllers

$$\frac{\theta_2(s)}{E(s)} = \frac{0.8}{s^3 + 8.3s^2 + 23.3s + 34.5}$$

Proposed controllers design

Augmentations of the model with weighting functions:

In this part, we will focus on the weighted control structure shown in Fig. 2 where $W_1(s)$, $W_2(s)$ and $W_3(s)$ are weighting functions or weighting filters. We assume that $G(s)$, $W_1(s)$ and $W_3(s)$ are all proper; i.e., they are bounded when $s \rightarrow \infty$. It can be seen that the weighting function $W_3(s)$ is not required to be proper. One may wonder why we need to use three weighting functions in Fig. 2. First, we note that the weighting functions are, respectively, for the three signals, namely, the error, the input and the output. In the two-port state space structure, the output vector $y1 = [y1a, y1b, y1c]^T$ is not used directly to construct the control signal vector $u2$. We should understand that $y1$ is actually for the control system performance measurement. So, it is not strange to include the filtered “input signal” $u(t)$ in the “output signal” $y1$ because one may need to measure the control energy to assess whether the designed controller is good or not. Clearly, Fig. 2 represents a more general picture of optimal and robust control systems. We can design an H_2 synthesis and H_∞ synthesis controllers by using the idea of the augmented state space model^[5].

The weighting function $W_1(s)$, $W_2(s)$ and $W_3(s)$ are chosen as:

$$W_1(s) = \frac{s+10}{10s+5} \quad W_2(s) = \frac{s+15}{2s+24} \quad W_3(s) = 10$$

The H_2 optimal controller become:

$$G_{ch_2} = \frac{0.05246s^4 + 1.064s^3 + 6.429s^2 + 16.46s + 21.75}{s^5 + 23.9s^4 + 162.1s^3 + 477.9s^2 + 757.8s + 278.2}$$

The H_∞ synthesis controller become:

$$G_{ch_\infty} = \frac{0.1408s^4 + 2.855s^3 + 17.26s^2 + 44.2s + 58.38}{s^5 + 23.91s^4 + 162.2s^3 + 478.2s^2 + 758.6s + 278.6}$$

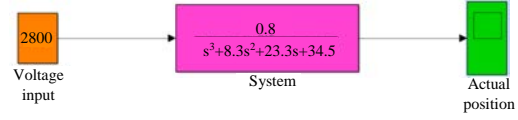


Fig. 3: Simulink model of the open loop system

Table 2: Step response data

Performance data	H_2 optimal	H_∞ synthesis controller
Rise time	1.4 (sec)	1.2 (sec)
Per. overshoot	3 (%)	13.8 (%)
Settling time	7 (sec)	12 (sec)
Peak value	65 (°)	74 (°)

RESULTS AND DISCUSSION

Open loop response of the vehicle boom barrier gate system:

The Simulink model of the open loop system is shown in Fig. 3. For the system output angular position to make a vehicle to pass through, it must be opened at least 65°. So, the voltage input becomes 2800 volt which is a high voltage and the system needs to improve the input voltage as shown in the simulation result in Fig. 4.

Comparison of the vehicle boom barrier gate system with H_2 optimal and H_∞ synthesis controllers using step input desired position signal:

The Simulink model of the vehicle boom barrier gate system with H_2 optimal and H_∞ synthesis controllers using step input desired position signal is shown in Fig. 5.

The simulation result of the comparison with the input voltage to the system with H_2 optimal and H_∞ synthesis controllers are shown in Fig. 6-8, respectively^[6].

The input voltages of the vehicle boom barrier gate system with the proposed controllers shows improvement in reducing the voltage amplitude but the system with H_2 optimal controller shows better improvement. The data of the rise time, percentage overshoot, settling time and peak value is shown in Table 2.

As Table 2 shows that the vehicle boom barrier gate system with H_2 optimal controller improves the performance of the system by minimizing the percentage overshoot and settling time.

Comparison of the vehicle boom barrier gate system with H_2 optimal and H_∞ synthesis controllers using operational open and close input desired position signal:

The Simulink model of the vehicle boom barrier gate system with H_2 optimal and H_∞ synthesis controllers using operational open and close input desired position signal is shown in Fig. 9.

The simulation result of the comparison with the input voltage to the system with H_2 optimal and H_∞ synthesis controllers are shown in Fig. 10-12, respectively.

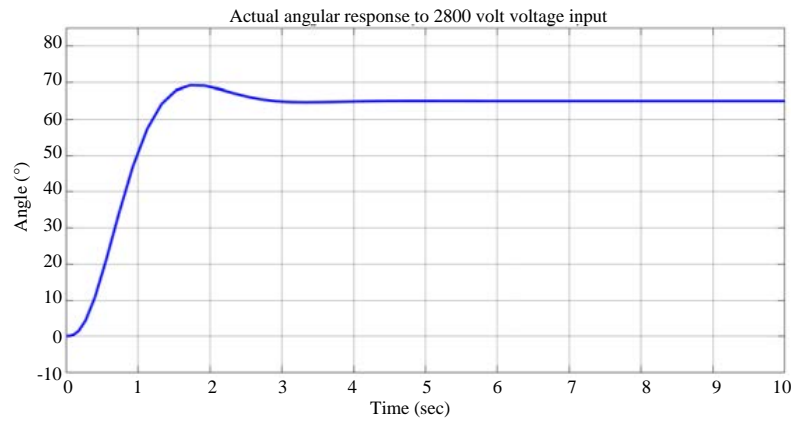


Fig. 4: Open loop simulation result

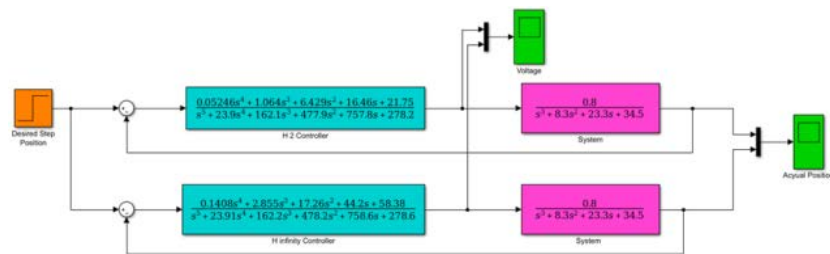


Fig. 5: Simulink model of the vehicle boom barrier gate system with H_2 optimal and H_∞ synthesis controllers using step input desired position signal

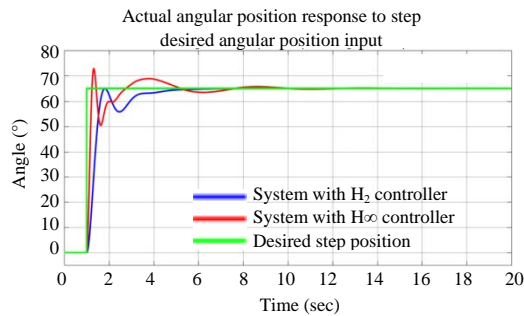


Fig. 6: Step response of the comparison

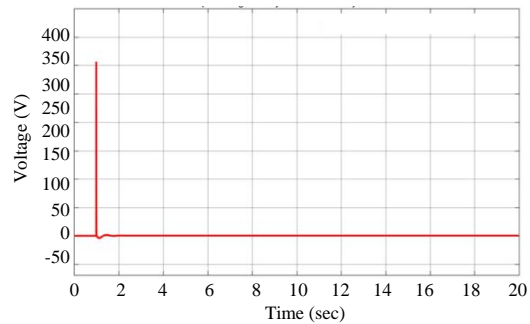


Fig. 8: Input voltage to the system with H_∞ synthesis controller

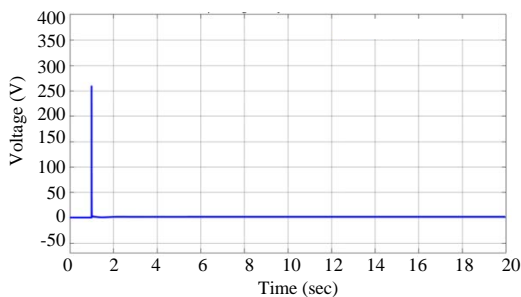


Fig. 7: Input voltage to the system with H_2 optimal controller

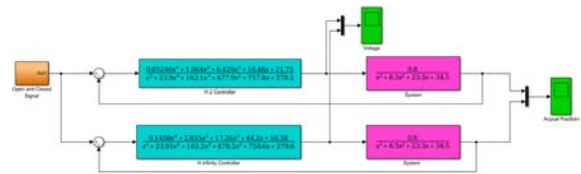


Fig. 9: Simulink model of the proposed system with H_2 optimal and H_∞ synthesis controllers using operational open and close input desired position signal

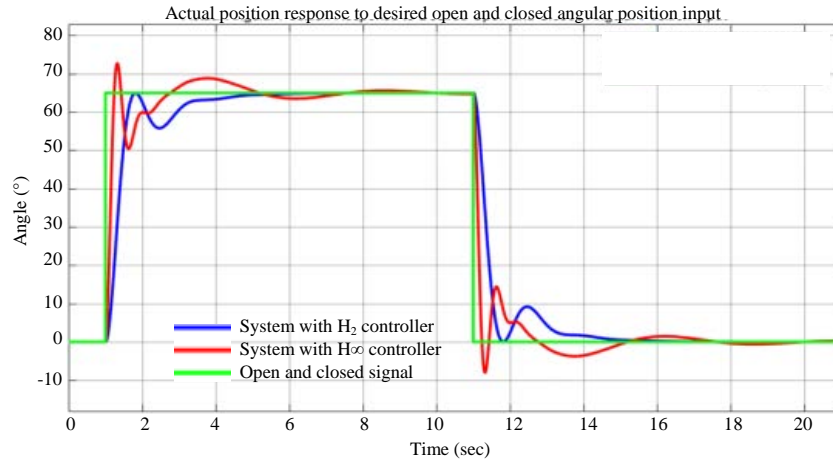


Fig. 10: Operational open and close response of the comparison

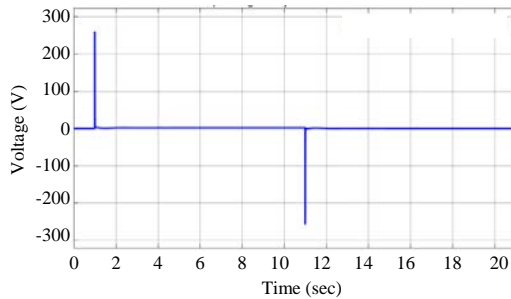


Fig. 11: Input voltage to the system with H_2 optimal controller

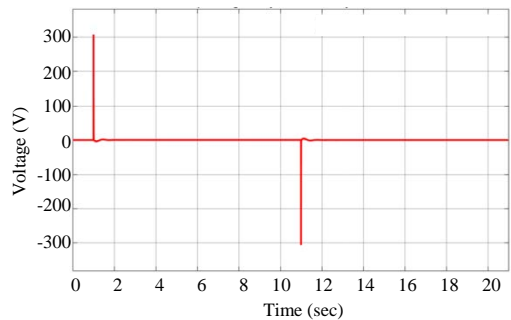


Fig. 12: Input voltage to the system with H_∞ synthesis controller

For the vehicle boom barrier gate system with H_∞ synthesis controllers, the system opens and closed with high oscillation and even not reaching the steady state value as compared to the system with H_2 optimal controller while the input voltages of the system with the proposed controllers shows improvement in reducing the voltage amplitude but the system with H_2 optimal controller shows better improvement^[7].

CONCLUSION

In this study, the design and control of a vehicle boom barrier gate system is done using Matlab/Simulink Toolbox using robust augmentation technique with H_2 optimal and H_∞ synthesis controllers successfully. The open loop response analysis of the system shows that the system must be opened at least 65° to pass a vehicle and the input voltage becomes 2800 volt which is a high voltage and the system needs to improve the input voltage. Comparison of the vehicle boom barrier gate system with H_2 optimal and H_∞ synthesis controllers have been done to track a set point using a step and operational open and close input signals. The step response shows that the system with H_2 optimal controller improves the performance of the system by minimizing the percentage overshoot and settling time while the response to the operational open and close input signal shows that the vehicle boom barrier gate system with H_∞ synthesis controller opened and closed with high oscillation and even not reaching the steady state value as compared to the system with H_2 optimal controller. Finally, the comparison simulation results proves the system with H_2 optimal controller improves the performance of the system.

REFERENCES

01. Kasym, K., A. Sarsenen, Z. Segizbayev, D. Junuskaliyeva and M.H. Ali, 2018. Parking gate control based on mobile application. Proceedings of the 2018 Joint 7th and 2nd International Conference on Informatics, Electronics & Vision and Imaging, Vision & Pattern Recognition (ICIEV) and (icIVPR), June 25-29, 2018, IEEE, Kitakyushu, Japan, pp: 399-403.

02. Kebiru, A. and E.O.M. Abdul-Wajid, 2017. Design and development of an automatic vehicle gate opener. *IOSR J. Eng. (IOSRJEN.)*, 7: 12-17.
03. Karlos, V., M. Larcher and G. Solomos, 2017. Review on vehicle barrier protection guidance. JRC Science for Policy Report, Publications Office of the European Union, Luxembourg.
04. Jonathan, A.E. and N.T. Michael, 2014. An electronically controlled automatic security access gate. *Leonardo J. Sc.*, 25: 85-96.
05. Li, C., 2013. Introduction to the design of the control system of the automobile in and out. *J. Wuxi Nanyang Vocational Coll.*, 6: 51-53.
06. Adewuyi, P.A., M.O. Okelola and A.O. Jemilehin, 2013. An intelligent gate controller using a personal computer and pattern recognition protocols. *Int. J. Comput. Intell. Inf. Secur.*, 4: 13-20.
07. Adewuyi, P.A., M.O. Okelola and A.O. Jemilehin, 2013. PIC based model of an intelligent gate controller. *Int. J. Eng. Adv. Technol.*, 2: 601-605.